Electronic Supplementary Material (ESI) for Journal of Materials Chemistry C.


# Supporting Information

## Ultrastretchable, Self-healable and Adhesive Composite Organohydrogels with Fast Response for Human-Machine Interface Application

Zhihui Xie[a], Zhuo Chen[a], Xiangshu Hu[a], Hao-Yang Mi[a,b], Jian Zou[a], Heng Li[c], Yuejun Liu[a], Zhi Zhang[d], Yinghui Shang[d], Xin Jing[a*]

[a]Key Laboratory of Advanced Packaging Materials and Technology of Hunan Province, Hunan University of Technology, Zhuzhou, 412007, China.

[b]Key Laboratory of Materials Processing and Mold, Zhengzhou University, Zhengzhou, 450000, China

[c]Department of Building and Real Estate, Hong Kong Polytechnic University, Hong Kong, 518000, China.

[d]Shenzhen Weijian Wuyou Technology, Shenzhen, Guangdong, China, 518102

**Corresponding Authors:**

Xin Jing

E-mail: jingxin@hut.edu.cn

**Table S1** Preparation of different hydrogels.

| Sample | Soaking solution | | Soaking time (h) |
|---|---|---|---|
| | LiCl (M) | $H_2O$/Elthyene glycol (v/v) | |
| PCH | - | - | - |
| PCOH-2 | 1 | 8:2 | 2 |
| PCOH-5 | 1 | 5:5 | 2 |
| PCOH-8 | 1 | 2:8 | 2 |

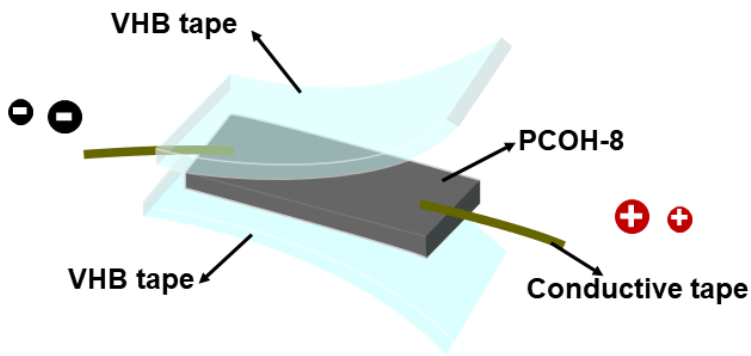


**Figure S1.** Schematic illustration of the sandwiched hydrogel strain sensor.

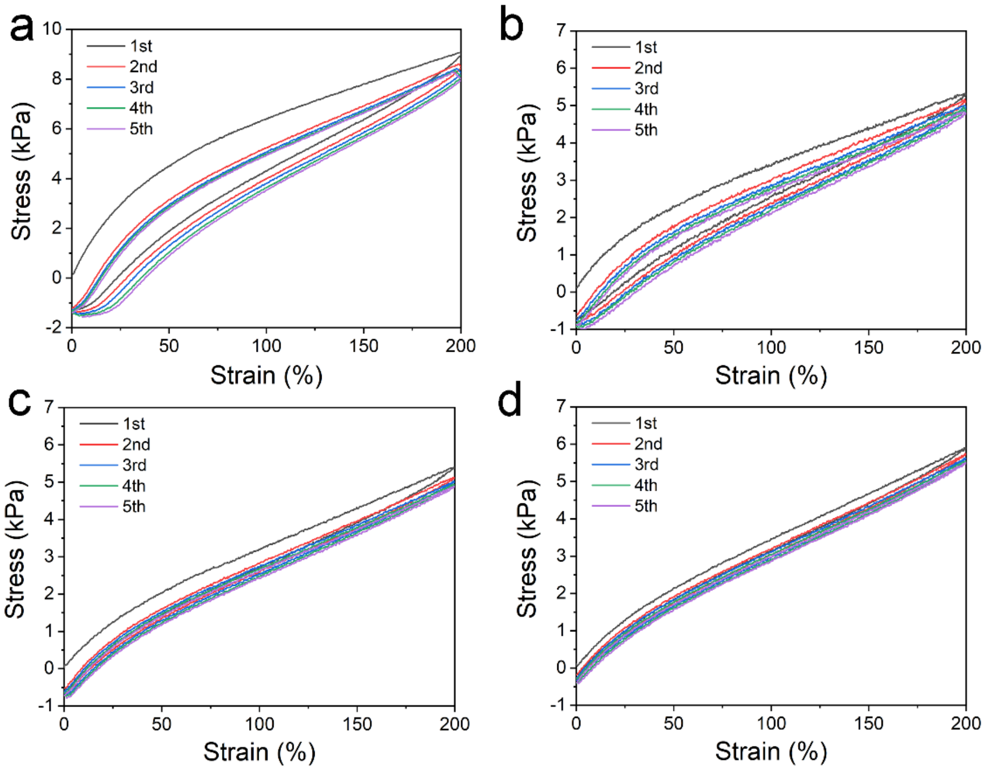


**Figure S2.** Strain-stress cyclic curves of (a) PCH; (b) PCOH-2; (c) PCOH-5; (d) PCOH-8.

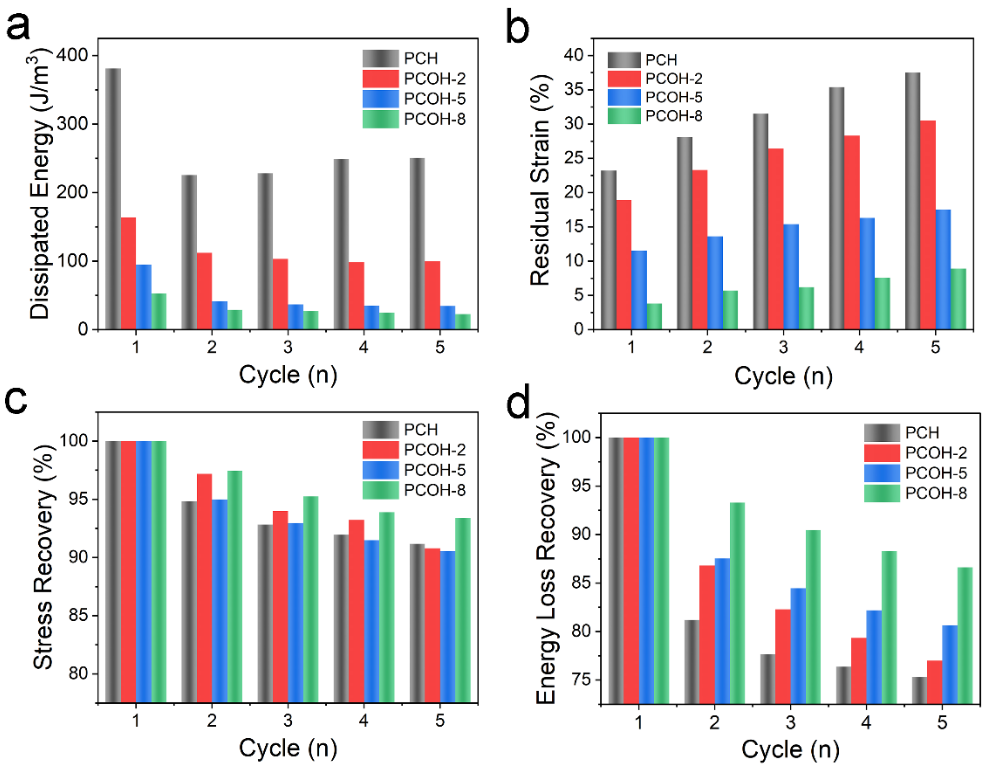


**Figure S3.** (a) The dissipated energy, and (b) The residual strain of successive cyclic tensile loading-unloading curves of PCH, PCOH-2, PCOH-5, and PCOH-8. (c) The stress recovery rates between the original and other cycles. (d) The energy loss recovery rates between the original and other cycles.

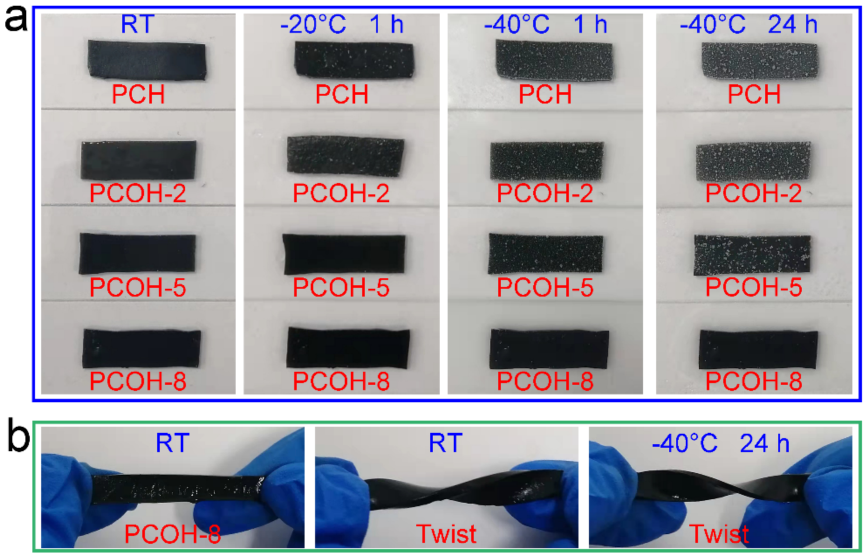


**Figure S4.** (a) Digital images of the hydrogel samples under different environments: room temperature, -20 °C for 1 h, -40 °C for 1h, and -40 °C for 24 h, respectively. (b) . Photographs of PCOH-8 upon being twisted at room temperature and at -40°C after storage for 24 h, respectively.

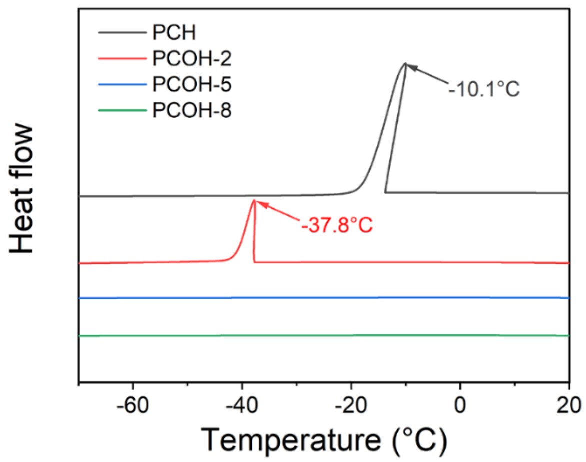


**Figure S5.** The DSC results of the PCH, PCOH-2, PCOH-5, and PCOH-8.

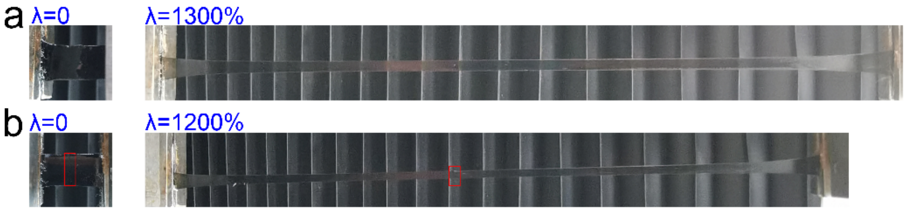


**Figure S6.** Photos of the PCOH-8 under stretching: (a) original PCOH-8 and (b) after self-healing for 2 h.

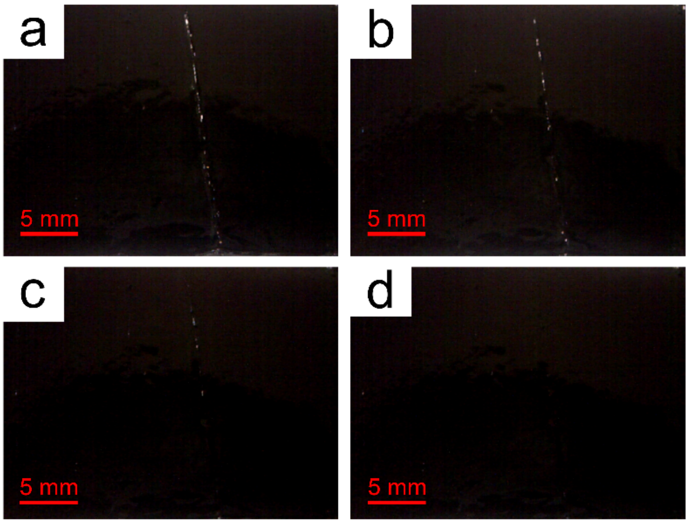


**Figure S7.** The self-healing behavior of the PCOH-8 upon different healing time. (a) 0 min, (b) 30 min, (c) 60 min and (d) 120min.

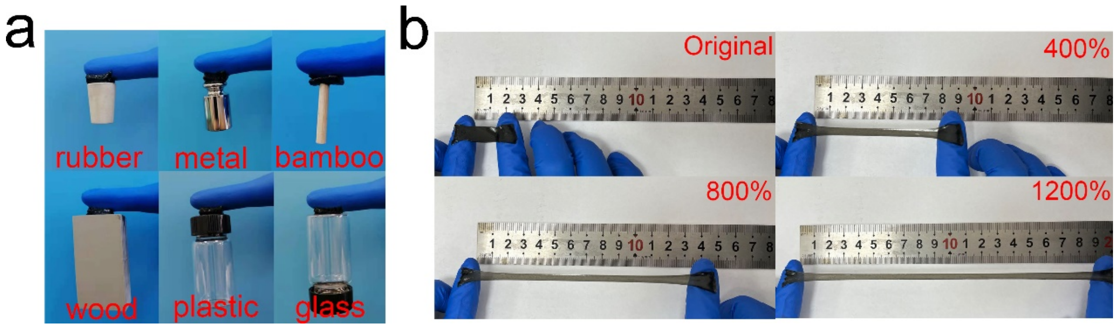


**Figure S8.** (a) Adhesion of the PCOH-8 to various substrates. (b) Optical images of the PCOH-8 adhered to nitrile gloves without the assistance of additional tape even under a stretch of 400%, 800%, and 1200%.

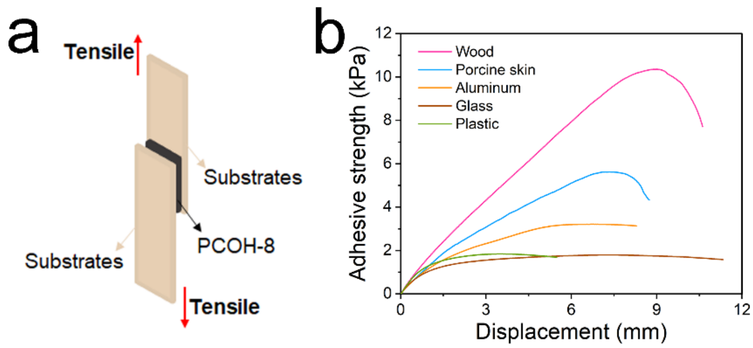


**Figure S9.** (a) Schematic of the adhesive tests on prepared PCOH-8. (b) Adhesive strength of PCOH-8 to diverse substrates (plastic, glass, aluminum, porcine skin and wood).

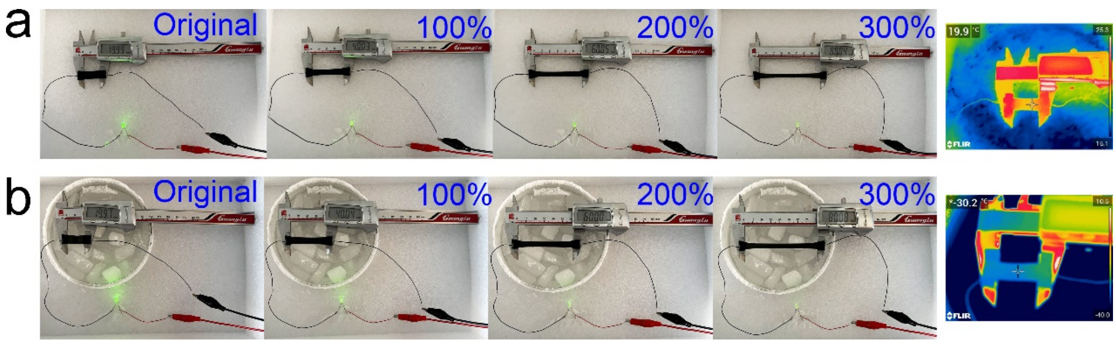


**Figure S10.** The conductive performance of PCOH-8 at different temperature: (a)room temperature; (b) -72°C.

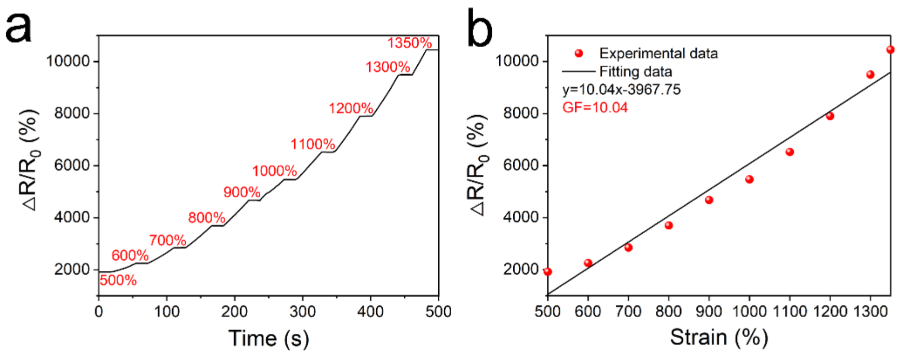


**Figure S11.** (a) Relative resistance change of the PCOH-8 being stretched for different strains. (b) GF of the PCOH-8 at different strains.

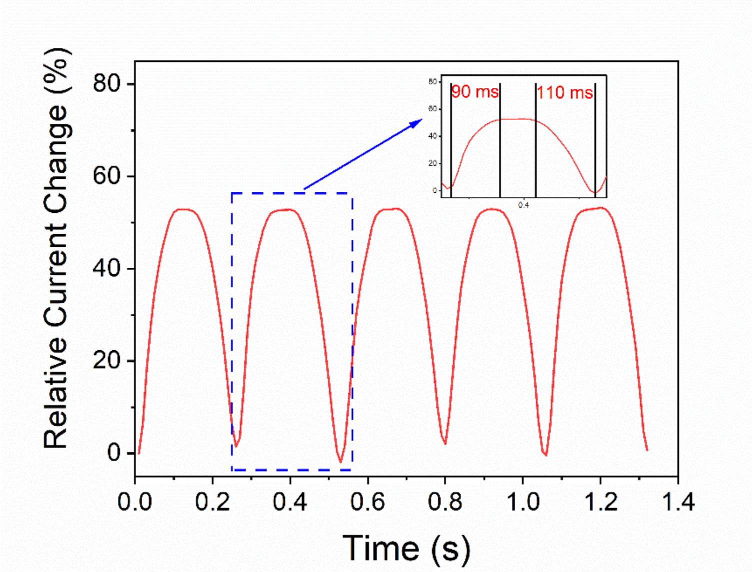


**Figure S12.** Response and release behavior of the strain sensor as the wrist bends.

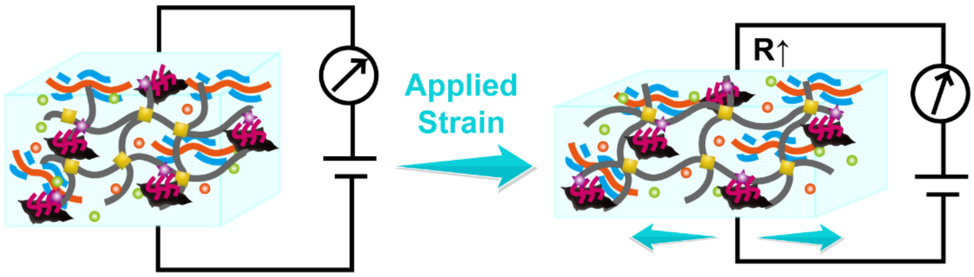


**Figure S13.** Scheme illustration of the strain sensing mechanism.

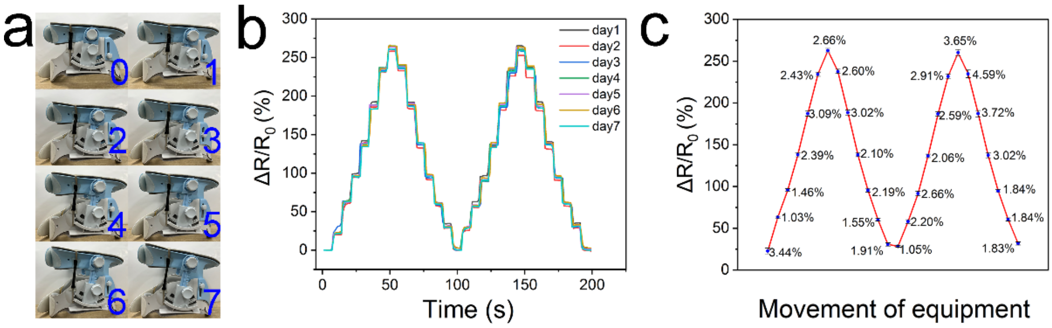


**Figure S14.** (a) The images of the PCOH-8 based strain sensor for detecting the up-down movement based on neck brace. (b) The long-term stability of the PCOH-8 based strain sensor for detecting the movement based on neck brace. (c) The error bar of each platform from b.

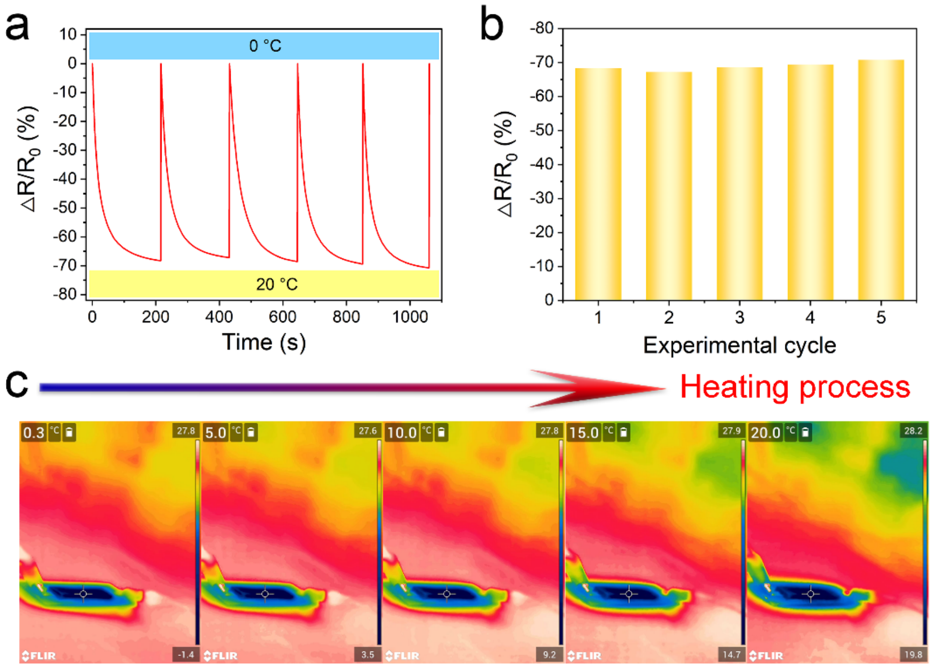


**Figure S15.** (a) Dynamic and quantitative responses of PCOH-8 from 0 to 25 °C for repeated five cycles. (b) The resistance changes corresponding to the repeated five cycles. (c) Infrared thermal images of PCOH-8 at 0 °C, 5 °C, 10 °C, 15 °C, and 20 °C, respectively.

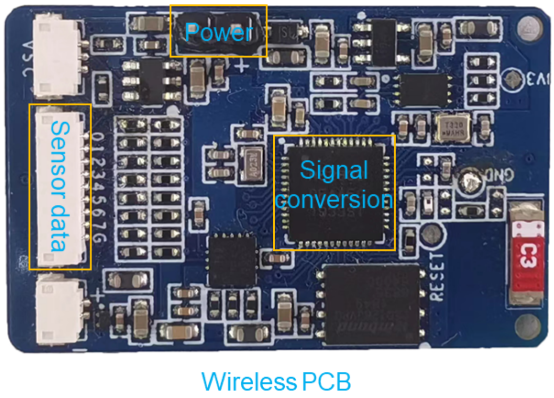


**Figure S16.** The module of signal processing-transmitting.

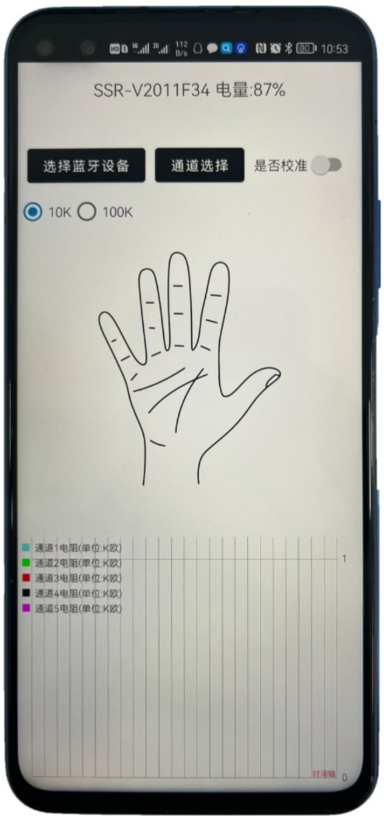


**Figure S17.** The interface of APP.

**Table S2.** Comparison in the properties of hydrogel based on different materials.

| Flexible sensor composition | Anti-freezing ability | Self-healing efficiency | Self-adhesion | Strain (%) | Ref. |
|---|---|---|---|---|---|
| **PDA-rGO/ PEDOT:PSS/PAM organohydrogel** | **-40 °C 24 h** | **tensile strength (92%); elongation at break (90%); electrical (90%)** | **YES** | **1350** | **This work** |
| PAM/gelatin/ PEDOT: PSS | - | - | NO | 2850 | Nano Energy, 2020 [1] |
| Alg-PBA/PVA /PAM/rGO | -40 °C, 24 h | elongation at break (90%) | NO | - | ACS Appl. Mater. Interfaces 2019 [2] |
| CDB/PAM/PEDOT: PSS | - | elongation at break (92%) | YES | 2763 | Chem. Eng. J., 2021[3] |
| PDA-rGO/ SA/PAM organohydrogel | -40 °C, 3 h | - | NO | 312 | J. Mater. Chem. C, 2021[4] |
| PEDOT:PSS-P(AAM-co-MAA) | - | - | YES | 129 | Colloids Surf. A Physicochem. Eng. Asp. , 2021[5] |
| PVA-MXene-PEDOT:PSS–PDA | - | tensile strength (88.56%); elongation at break (95.47%) | YES | 650 | J. Mater. Chem. A, 2021[6] |

**Table S3.** Comparison in the properties and applications of hydrogel-based strain sensors based on Table S2.

| **Flexible sensor composition** | **Response time (ms)** | **Sensitivity** | **Human motion detection** | **Ref.** |
|---|---|---|---|---|
| **PDA-rGO/ PEDOT:PSS/PAM organohydrogel** | **90** | **0-500%, 3.91; 500%-1350%, 10.04** | **finger bending; wrist bending; knee bending; cheek-bulging; fowrn; opening mouth** | **This work** |
| PAM/gelatin/ PEDOT: PSS | 200 | 0-2850%, 1.58 | cheek-bulging; eyebrow up-down; finger bending; elbow bending; knee bending; | Nano Energy, 2020 [1] |
| Alg-PBA/PVA /PAM/rGO | 100 | - | finger bending; elbow bending; swallowing; speaking | ACS Appl. Mater. Interfaces 2019 [2] |
| CDB/PAM/PEDOT: PSS | - | - | finger bending | Chem. Eng. J., 2021[3] |
| PDA-rGO/ SA/PAM organohydrogel | 200 | 0-250%, 2.09 | finger bending; elbow bending; cheek-bulging; fowrn; a tiny breathing | J. Mater. Chem. C, 2021[4] |
| PEDOT:PSS-P(AAM-co-MAA) | - | 0-70%, 0.003 | - | Colloids Surf. A Physicochem. Eng. Asp. , 2021[5] |
| PVA-MXene-PEDOT:PSS-PDA | 630 | 0-500%, 2.55 | finger bending; wrist bending; winking; smile | J. Mater. Chem. A, 2021[6] |

**Table S4**. Summary of thermosensation capacities of hydrogel-based temperature sensors.

| Materials | TCR (%/°C) | Sensing range (°C) | Ref. |
|---|---|---|---|
| **PDA-rGO/ PEDOT:PSS/PAM organohydrogel** | **127.54 (-20~ -40 °C)**<br>**42.21 (-5~ -20 °C)**<br>**11.93 (15~ -5 °C)**<br>**1.64 (15~ 60 °C)** | **-40~60** | **This work** |
| PANI NFs/PAA/$Fe^{3+}$ | 1.64 | 40~110 | ACS Nano, 2020[7] |
| PVA/DMSO/rGO/GO organohydrogels | 3.81 | 20~85 | J. Mater. Chem.A, 2021[8] |
| PNIPAM/PEDOT:PSS/CNT | 2.6 | 25~40 | ACS Appl Mater Interfaces, 2018 [9] |
| PVA/Gly/CB/CNT organohydrogel | 0.935 | 30~80 | ACS Appl Mater Interfaces, 2020[10] |
| PAA-NCT | 252 (-35~ -30 °C)<br>28.7 (-30~ -5 °C)<br>1.78 (5~ 20 °C)<br>1.89 (20~ 50 °C) | -35~50 | ACS Sustain. Chem. Eng., 2021[11] |
| P(AAm-AAc) | 2.89 | 15~40 | Adv. Funct. Mater., 2021[12] |
| PVA/CNFs organohydrogels | 15 (0~ -30 °C)<br>45 (20~ 0 °C)<br>2.14 (20~ 34 °C)<br>0.944 (34~ 53 °C)<br>0.471 (53~ 70 °C) | -30~70 | J. Mater. Chem.A, 2020[13] |

The sensitivity in the above table is defined as $\Delta G/G_0/\Delta T$ or $\Delta R/R_0/\Delta T$.

## References


1. H. Sun, Y. Zhao, C. Wang, K. Zhou, C. Yan, G. Zheng, J. Huang, K. Dai, C. Liu and C. Shen, *Nano Energy*, 2020, **76**, 105035.
2. D. Ma, X. Wu, Y. Wang, H. Liao, P. Wan and L. Zhang, *ACS Appl Mater Interfaces*, 2019, **11**, 41701-41709.
3. M. Suneetha, O. Sun Moo, S. Mo Choi, S. Zo, K. Madhusudana Rao and S. Soo Han, *Chemical Engineering Journal*, 2021, **426**, 130847.
4. Z. Xie, H. Li, H.-Y. Mi, P.-Y. Feng, Y. Liu and X. Jing, *Journal of Materials Chemistry C*, 2021, **9**, 10127-10137.
5. F. Sun, X. Huang, X. Wang, H. Liu, Y. Wu, F. Du and Y. Zhang, *Colloids and Surfaces A: Physicochemical and Engineering Aspects*, 2021, **625**, 126897.
6. W. Zhao, D. Zhang, Y. Yang, C. Du and B. Zhang, *Journal of Materials Chemistry A*, 2021, **9**, 22082-22094.
7. G. Ge, Y. Lu, X. Qu, W. Zhao, Y. Ren, W. Wang, Q. Wang, W. Huang and X. Dong, *ACS Nano*, 2020, **14**, 218-228.
8. H. Chen, J. Huang, J. Liu, J. Gu, J. Zhu, B. Huang, J. Bai, J. Guo, X. Yang and L. Guan, *Journal of Materials Chemistry A*, 2021, **9**, 23243-23255.
9. J. H. Oh, S. Y. Hong, H. Park, S. W. Jin, Y. R. Jeong, S. Y. Oh, J. Yun, H. Lee, J. W. Kim and J. S. Ha, *ACS Appl Mater Interfaces*, 2018, **10**, 7263-7270.
10. J. Gu, J. Huang, G. Chen, L. Hou, J. Zhang, X. Zhang, X. Yang, L. Guan, X. Jiang and H. Liu, *ACS Appl Mater Interfaces*, 2020, **12**, 40815-40827.

11. X. Jing, P. Feng, Z. Chen, Z. Xie, H. Li, X.-F. Peng, H.-Y. Mi and Y. Liu, *ACS Sustainable Chemistry & Engineering*, 2021, **9**, 9209-9220.

12. T. H. Park, S. Park, S. Yu, S. Park, J. Lee, S. Kim, Y. Jung and H. Yi, *Adv Healthc Mater*, 2021, **10**, e2100469.

13. X. Pan, Q. Wang, R. Guo, S. Cao, H. Wu, X. Ouyang, F. Huang, H. Gao, L. Huang, F. Zhang, L. Chen, Y. Ni and K. Liu, *Journal of Materials Chemistry A*, 2020, **8**, 17498-17506.